

# ON CROSS-TALK CORRECTION OF IMAGES FROM MULTIPLE-PORT CCDS\*

L. M. FREYHAMMER<sup>1,2\*</sup>, M. I. ANDERSEN<sup>3</sup>, T. ARENTOFT<sup>1,2</sup>, C. STERKEN<sup>2</sup> and  
P. NØRREGAARD<sup>4</sup>

<sup>1</sup> *Royal Observatory of Belgium, Brussels, Belgium.*

<sup>2</sup> *University of Brussels (VUB, OBSS/WE), Brussels, Belgium.*

<sup>3</sup> *Division of Astronomy, University of Oulu, Finland.*

<sup>4</sup> *NBI/AFG, Astronomical Observatory, Copenhagen Ø, Denmark*

(\* author for correspondence, e-mail: lfreyham@vub.ac.be)

(Received 11 February 2002; accepted 15 July 2002)

**Abstract.** Multi-channel CCD read-out, which is an option offered at most optical observatories, can significantly reduce the time spent on reading the detector. The penalty of using this option is the so-called amplifier cross-talk, which causes contamination across the output amplifiers, typically at the level of 1:10 000. This can be a serious problem for applications where high precision and/or high contrast is of importance. We represent an analysis of amplifier cross-talk for two instruments – FORS1 at the ESO VLT telescope Antu (Paranal) and DFOSC at the Danish 1.54 m telescope (La Silla) – and present a post-processing method for removing the imprint of cross-talk. It is found that cross-talk may significantly contaminate high-precision photometry in crowded fields, but it can be effectively eliminated during data reduction.

**Keywords:** amplifier, cross-talk, detection: CCD, instrumentation: high-precision photometry

## 1. Introduction

Reading out charge-coupled devices (CCDs) with low noise contributions from the electronics chain has its costs: read-out times that may consume several minutes of precious observing time for the detector systems commonly in use. When read-out time is comparable to the integration time, the advantage of reading out the CCD through multiple ports is obvious: for time-series observations the temporal resolution may be more than doubled.

Most modern CCDs have two or four output amplifiers, which can reduce the read-out time twofold or fourfold when operated in parallel. Unfortunately, it is almost unavoidable that the CCD and/or the associated read-out electronics induce a *cross-talk signal* between the amplifiers during simultaneous clocking operations. Thus, when a bright source is present in one half (or quadrant, in the case of a CCD with four read-out channels), a *ghost* image (or images) appears in the other half

\* Based on observations obtained at the European Southern Observatory at Paranal and La Silla, Chile (Applications 63.L-0686(A) and D1.54, Danish time).



(or quadrants) of the CCD, at a position mirrored over the border between the read-out regions. The cross-talk signal may be positive or negative (see e.g. Marshall, 1995) and typically, for the CCD systems we have tested, has an amplitude of about +1 part in 10 000 or  $10^{-4}$  of the image producing the ghost. This effect is quite undesirable for high-precision photometry in crowded fields and may also be a problem for deep imaging and for spectroscopy.

Several of our projects concern time-series photometry of variable stars in star clusters (see e.g. Arentoft et al., 2001; Freyhammer et al., 1999). In order to avoid spending the majority of the observing time on CCD read-out, the detector is read out using the available amplifiers. As some stars in our fields are considerably brighter than the stars we are investigating, amplifier cross-talk becomes a matter of concern.

This article describes a procedure to measure cross-talk inside and beyond the camera's digital range. We apply the procedure on scientific data, remove the cross-talk contamination and analyse the effects on time-series photometry. Limitations of the procedure are discussed.

## 2. Theoretical background

Read-out procedures of CCDs have been thoroughly described in the literature (e.g. Mackay, 1986; McLean, 1997) and will not be repeated here. A brief description of the procedure is: while exposing, the incident photon flux is converted to photoelectrons, which are collected in the individual pixel potential wells. During read-out the charge of each pixel is passed sequentially to an on-chip output amplifier via the parallel and serial registers. The on-chip amplifier, which has a very low noise on scientific CCDs (a few  $e^-$ , see also Mackay et al., 2001), then converts the charge packet to a voltage. This voltage is subsequently amplified further by an off-chip amplifier, before being converted to digital units by an *analog-to-digital* converter (ADC).

In the digitisation process four factors are important:

1. *System gain* ( $q$ ) expresses the number of electrons represented by each count (ADU, *Analog-to-Digital Unit*) by the ADC.
2. *Read-out noise* of which there are two types: a digitisation noise of  $0.29 q$  (McLean, 1997) and a random electronic noise from the CCD on-chip amplifier. Novel CCD architectures provide CCD cameras with virtually no read-out noise (Mackay, 2001).
3. *Pixel full-well capacity* (hereafter full well) is the number of electrons a pixel can hold before the charges escape the potential barriers and spill over into adjacent pixels in the column.
4. *Numerical saturation limit* is the ceiling of the digital counts from the ADC, mostly 16 bit ( $2^{16} - 1$  or 65 535 ADU).

The choice of the gain is important; it is typically adjusted so the read-out noise corresponds to 2.5–4 ADU. This setting is designed as a balance of chiefly sampling the read-out noise and to optimally utilise the pixel well while safeguarding the scientific application of the camera. In this more concerns partake: The *system dynamic range* should be as high as possible. It is defined as the ratio of the brightest and the faintest signal detectable, which for a CCD is the ratio of the full-well to read-out noise. One may also define a ‘net dynamic range’ as the saturation limit to noise ratio. For a *low gain* (i.e. more  $e^-$  per ADU) the pixel well can be fully utilised and digitally represented before numerical saturation occurs. But only at the cost of a higher digitisation noise, because the read-out noise becomes under-sampled (units of gain are larger than the noise). A low gain is, therefore, suited for scientific observations in stellar fields, where bright sources would otherwise quickly fill the pixel wells and cause charge bleeding, or when observing multiple astronomical targets covering a large magnitude range. In the low gain mode will the net dynamic range be limited by the read-out noise at low light levels and by photon counting noise at high light levels. On the other hand, a *high gain* (e.g. 0.5  $e^-$  per ADU) gives minimal digitisation noise, but only a small part of the well is utilised. This is ideal for applications with low level signals, such as most astronomical applications, but bright targets will quickly saturate. The common solution is to offer the user a high and a low gain level, switchable in the software.

A CCD camera with the gain adjusted to exclude full well from the ADC’s digital range is nominally linear until the ADC saturates. Above numerical saturation, the CCD output is still proportional to the photon flux until the pixel wells are almost full. Then, the total stored charge can effect the electric potential of the applied clock voltage and degrade the charge transfer (i.e. *Charge-Transfer Efficiency*, CTE) or coupling (McLean, 1997). At full well, effects are seen around saturated pixels as vertical blurring (blooming) caused by the charge spilling. A pixel’s full well is typically  $700 e^- \mu\text{m}^{-2}$  and can be as high as  $900 ke^- \text{pixel}^{-1}$ , and may be increased electronically depending on the CCD design. The full well limits the maximum CCD output and by that it defines an upper limit on cross-talk.

Cross-talk occurs on the CCD chip itself, in the electronic board or in a combination of both. Possible sources for cross-talk can be non-zero dynamic impedance in CCD drain supplies, the wiring system adopted (common substrate, wires between output ports, insufficiently bypassed power supplies) and ADCs sharing common voltage supply (e.g. Hoffberg, 1997; Jorden, 1997). Cross-talk originating from electronic boards will remain after upgrades of the CCD and can be stable year after year (see e.g. Marshall, 1995).

Most CCD manufacturers reduce the cross-talk to an amplitude of  $10^{-4}$ , or 1 part in 10 000, e.g. by electronic shielding and adjusting supply voltages to the ADC. Cross-talk signal at this level becomes detectable in a sky background of 100 ADU per pixel when the ADC saturates, but will contribute until pixel full well is reached. The contamination may therefore become several times higher than the  $7 \text{ADU pixel}^{-1}$  at numerical saturation.

TABLE I  
Basic data for the two tested CCD cameras

Instrument	DFOSC	FORS1
Identification	W7-(0,0), Loral/Lesser	TK2048EB4-1, Tektronix
Controller	Copenhagen <sup>a</sup>	FIERA
Pixels	2048 × 2048, 15 μm	2048 × 2048, 24 μm
Full well	~118 000 e <sup>-</sup> pixel <sup>-1</sup>	~350 000 e <sup>-</sup> pixel <sup>-1</sup>
Non-linearity (r.m.s.)	<0.2%	<0.8%
Amplifiers	2 (A/B)	4 (A/B/C/D) <sup>b</sup>
Gain, (e <sup>-</sup> ADU <sup>-1</sup> )	1.37/1.27	2.90/3.50/3.08/3.22
Read-out noise, (e <sup>-</sup> )	7.7/9.57 (high gain, mpp-)	5.75/6.30/5.93/5.75 (low gain)

<sup>a</sup> For DFOSC cameras see <http://www.astro.ku.dk/~ijaf/>.

<sup>b</sup> Respectively located at CCD corners (1, 1), (2 k, 1), (1, 2 k) and (2 k, 2 k).

### 3. Observations and cross-talk measurements

The procedure to measure cross-talk is to illuminate each amplifier's CCD quadrant/half separately with a bright spot using a stable light source. This can be acquired in daytime on re-imaging instruments\* with a calibration lamp or dome light combined with a mask in the telescope focal plane. Instruments without similar options will have to be tested in nighttime with a single star serving as the light source. In principle a field with a few bright stars imaged on all amplifier CCD sections would give similar results. To obtain a high S/N ratio for the faint ghost image in the contaminated CCD-section, several images are needed for stacking purpose. Furthermore, to examine cross-talk in the region above numerical saturation, saturated as well as non-saturated images are needed from different exposure times.

Cross-talk measurements were obtained on the re-imaging instruments DFOSC, at the Danish 1.5 m telescope on La Silla and FORS1 at the ESO VLT telescope Antu on Paranal, in 1998 and 1999, respectively. Table I lists the properties of the two cameras used.

DFOSC\*\* is a focal-reducer instrument capable of spectroscopy and imaging. The camera (Table I) was equipped with a backside illuminated Ford-Loral CCD. Reading out with 2 amplifiers halved the read-out time to 45 s, but a known problem for the CCD (Sørensen and Andersen, 1997) is cross-talk with an amplitude of about 10<sup>-4</sup>. Because of this, we decided to measure the cross-talk ourselves and if possible correct for it. 'Bright spots' on the CCD were produced by a pinhole

\* Instruments designed such that any mask/slit placed in the telescope focal plane, is imaged onto the detector, usually with different plate scale (effective focal length).

\*\* See ESO manual <http://www.ls.eso.org/lasilla/Telescopes/2p2T/D1p5M/>

array in the aperture wheel located in the telescope focal plane, illuminated by a calibration lamp. Alternately, we covered pinholes projecting light on one of the CCD halves. Two series of ten exposures were obtained at  $0.5\times$  and  $5.0\times$  numerical saturation (65 535 ADU). The images in each series were then combined and background signal from stray light and optical reflections was removed with a median filter.

FORS1 is quite similar to DFOSC in functionality (but scaled up for an 8 m telescope) and is equipped with a Tektronic CCD detector (Table I). ESO estimates (ODT Team, private commun.) full well to about  $350\text{ ke}^-$ , in agreement with a value of  $343\text{ ke}^-$  found for another  $24\text{ }\mu\text{m}$  pixel Tektronix CCD that we measured at the Nordic Optical Telescope, La Palma. For our science observations we used all 4 amplifiers at the CCD corners, to read out the images, which reduced the read-out time to 25 s. As we optimised exposure times for the faint stellar population in a galactic star cluster, we anticipated extensive saturation in 1–2 per mille of the pixels and cross-talk was therefore measured.

We would have needed 4 times 20 images to map the 12 combinations of amplifier pairs individually: ten images per amplifier to increase S/N and at two different exposure levels. We simplified this by using a multi-object spectroscopy (MOS) mask to provide slit images in each quadrant. Care was taken to avoid cross-talk ghosts and slit images from coinciding. A constant illumination level was provided by flatfielding lamps, and three series of 10 images were obtained at  $0.4\times$ ,  $1.4\times$  and  $5.0\times$  full-well light-levels. The last series was obtained 12 h after the other two, but the flux was found to be the same to within 5% r.m.s. The three series were combined to three images according to exposure levels, like for the DFOSC data.

The images have variable high background from light entering between the MOS panels (Figure 6) and from optical reflections of the slit images. Median-smoothed images failed to properly remove the background of the ghost images, and local backgrounds were measured instead (see Section 4.2). The  $1.4\times$  and  $4\times$  full-well frames suffer from vertical charge blooming in the slit images. The  $5\times$  full-well image furthermore suffers from 5–10% fringing and bad CTE, why only small sections could be used for cross-talk measurements.

#### 4. Mapping of the cross-talk contribution

To determine the true signal  $N_B$  in a contaminated pixel in CCD section B, we must subtract the measured counts  $N'_B$  by the cross-talk signal  $N_{\text{CT}}(\text{AB})$  from the contaminating pixel in section A:

$$N_B = N'_B - N_{\text{CT}}(\text{AB}) . \quad (1)$$

If we assume linearity up to full well between  $N_{CT}(AB)$  and counts in channel A,  $N_A$ , then cross-talk amplitude  $CT(AB)$  follows from:

$$N_{CT}(AB) = N_A \times CT(AB) . \quad (2)$$

Thus, by subtracting the background counts from our calibration images, we eliminate  $N_B$  in Equation (1) and get:

$$N'_B = N_A \times CT(AB) . \quad (3)$$

In the following, we will measure  $N'_B$  and determine the cross-talk amplitudes between all amplifier pairs.

#### 4.1. TWO PORTS – DFOSC

The DFOSC camera's numerical saturation limit is 65 535 ADU and the CCD is nominally linear up to this value. Diffraction of the light through the pinholes gives a point-spread-function (PSF) distribution of intensity, with maximum in the center and decreasing with radial distance, which makes it possible to map cross-talk contribution for a continuous range of input flux.

In the following, the cross-talk signal from port A to port B is referred to as the  $AB$  term, and  $BA$  for the reverse direction. The non-saturated image (see Section 3) is scaled with exposure time to the illumination level of the saturated image, assuming full linearity and no blooming. For a stable light source this provides a realistic estimate of the illumination level in the saturated image, but not of the voltage entering the ADC because of non-linearity and a poor CTE in this region. Counts in the scaled A-section's pixels are then compared with the corresponding mirrored pixels' counts in the saturated image's B-section, as plotted in Figure 1 (top panel) and reverse (bottom panel).

Ghost images of pinhole images with charge blooming have elongated shapes unlike the circular shapes in the scaled non-saturated image. We therefore only measured counts in the core-regions of ghosts and scaled pinhole images.

Figure 1 shows the cross-talk vs. exposure level measurements, below and above numerical saturation for both cross-talk terms. The cross-talk signal is nominally linear almost up to 80 kADU (full-well capacity level) and then constant (20 ADU) for both ports. The AB and BA cross-talk contributions were fitted on both sides of full well with two piecewise linear functions, given with  $1-\sigma$  uncertainty estimates:

$$N_{CT}(AB) = \begin{cases} 2.3 \pm 0.1 \times 10^{-4} \times N_A & , N_A < 65\,535 \text{ ADU} \\ 20.0 \pm 0.8 & , N_A \geq 65\,535 \text{ ADU} \end{cases} \quad (4)$$

$$N_{CT}(BA) = \begin{cases} 2.5 \pm 0.1 \times 10^{-4} \times N_B & , N_B < 65\,535 \text{ ADU} \\ 20.0 \pm 0.6 & , N_B \geq 65\,535 \text{ ADU} \end{cases} \quad (5)$$

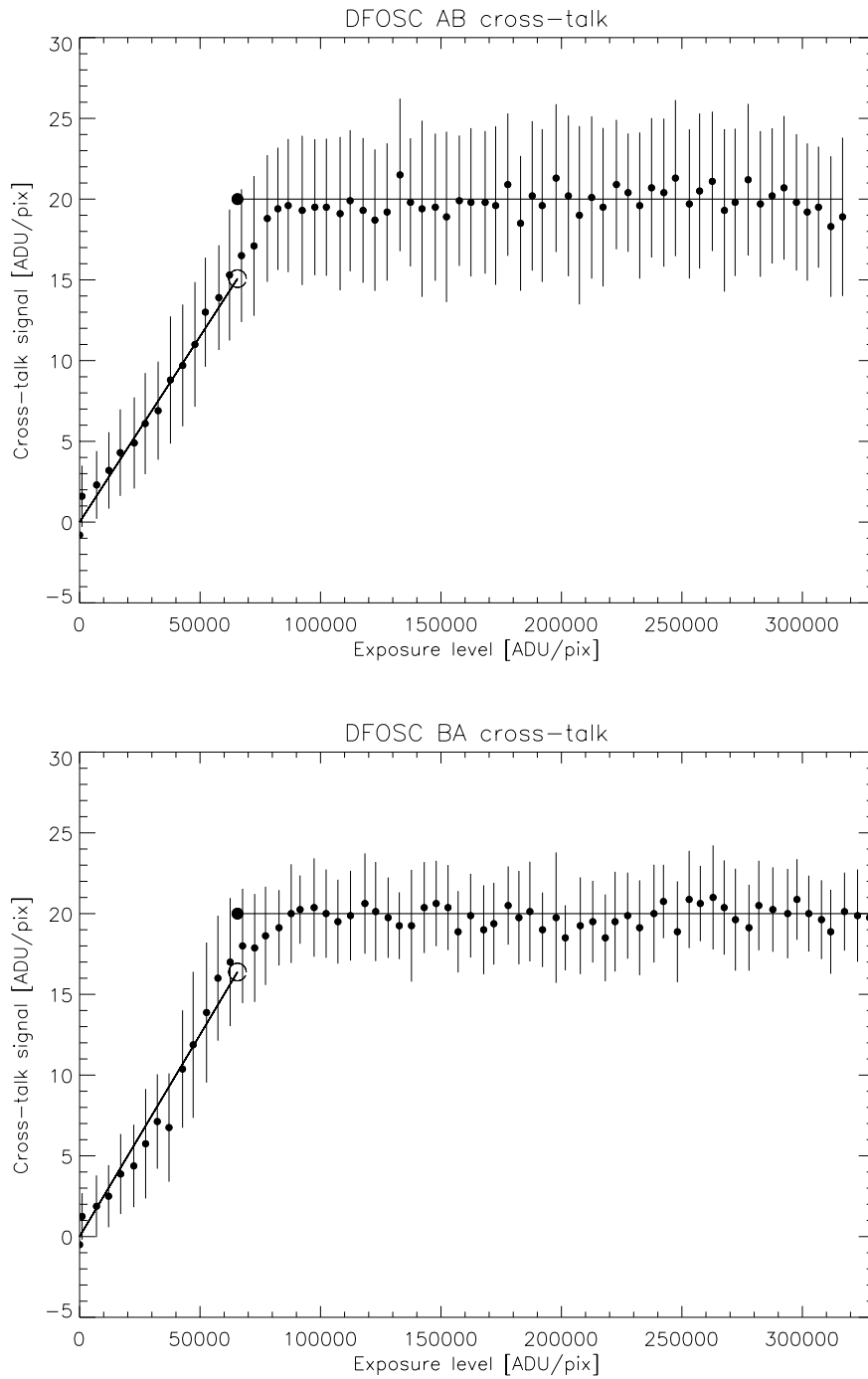


*Figure 1.* Cross-talk signal vs. exposure level measurements from DFOSC. Given as median values in bins of 5 kADU with  $1\text{-}\sigma$  errors indicated with error bars. Top: Cross-talk signal in port B versus illumination level in port A. Bottom: The same measurements, but for port A versus B. Piecewise functions (Equations (4) and (5)) to be used for recovering science images are superimposed.

TABLE II

Measured cross-talk amplitudes for the FORS1 CCD given as the ratio between cross-talk signal and exposure level at full-well capacity (122 kADU). Measurement accuracy is about  $1 \times 10^{-5}$

Source amplifier	Cross-talk amplitudes ( $10^{-5}$ )			
	A	B	C	D
A		12	1	1
B	1		3	<1
C	<1	1		<1
D	2	<2	1	

For practicality, the piecewise functions are defined to split at numerical saturation as one cannot measure above this value in science images. The resulting jump of 3–4 ADU limits the data correction, however in this case only with a minor error. Equations (4) and (5) were eventually used to estimate and remove cross-talk from science data *before bias* subtraction and flatfielding. Flatfields and bias images do not need any correction as the signal read out in all amplifiers is equivalent and the corresponding cross-talk signal is much less than a per mille of that.

#### 4.2. 4 PORTS – FORS 1

The cross-talk ghost images in the three combined images (see Section 3) are hampered by a variable high background level of 20–30 ADU, exceptionally up to 130 ADU, from optical reflections and stray light, so only parts of them can be used for reliable measurements. We enhanced, therefore, the S/N ratio for the contamination by measuring median pixel counts in 100 pixel<sup>2</sup> sections, while carefully avoiding regions with such background structures.

Cross-talk amplitudes for all terms were measured in the two saturated images as maximum ghost amplitude above the local background, corresponding to cross-talk at full-well signal. Table II gives the measured cross-talk amplitudes. Strongest is the AB term with an amplitude of  $10^{-4}$ , while all other terms are of the order of  $10^{-5}$  or less, including the diagonal terms AD, DA, BC and CB.

A detailed mapping of the AB cross-talk was made with all three images, using exposure levels scaled according to exposure time for the saturated images, and is shown in Figure 2. Like for the DFOSC CCD, the cross-talk increases linearly up to the full well (122 kADU) and is then constant. The relation is fitted by a piecewise function as shown in Figure 2 with a dotted line. Cross-talk contamination at numerical saturation is 8 ADU pixel<sup>-1</sup>, but the immeasurable range up to full well may contribute an additional 7 ADU pixel<sup>-1</sup>. From the distribution of pixel

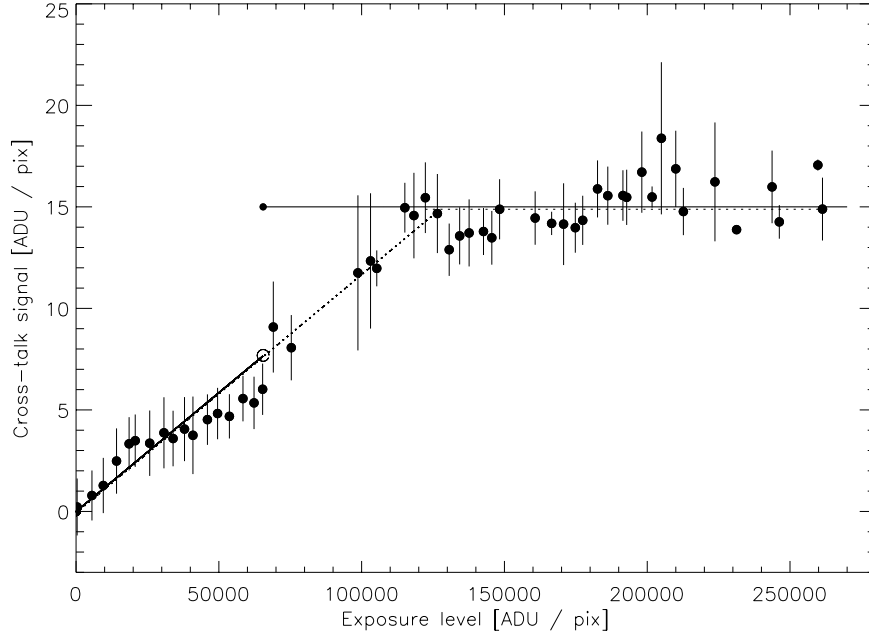


Figure 2. Cross-talk contribution from A to B amplifier, mapped for the FORS1 CCD. All three calibration images were used. The dotted line shows a fit to the data, and the thick lines show the function adopted for correcting science images.

counts in our science images we find that most saturated pixels are exposed to full well. We, therefore, fix the cross-talk contribution to  $15 \text{ ADU pixel}^{-1}$  at numerical saturation, and use the following function (Figure 2, solid lines) to recover the contaminated science data:

$$N_{\text{CT}}(\text{AB}) = \begin{cases} 1.17 \times 10^{-4} \times N_A & , N_A < 65\,535 \text{ ADU} \\ 15.0 & , N_A \geq 65\,535 \text{ ADU} \end{cases} \quad (6)$$

## 5. Results of the correction

To quantify the effect of the cross-talk correction, we reduced 108 DFOSC images of the open star cluster NGC6231 (Arentoft et al., 2001), all obtained during a single night, with and without applying the correction in Equations (4) and (5).

The observed field has several saturated stars, and strong vertical blooming produces cross-talk ghosts across the CCD halves as seen in Figure 5 (below). Differential photometry was made using the MOMF software (see Kjeldsen and Frandsen, 1992), which applies a combination of PSF and aperture photometry. The weather was stable and the photometry reaches an r.m.s. scatter of 1 mmag for

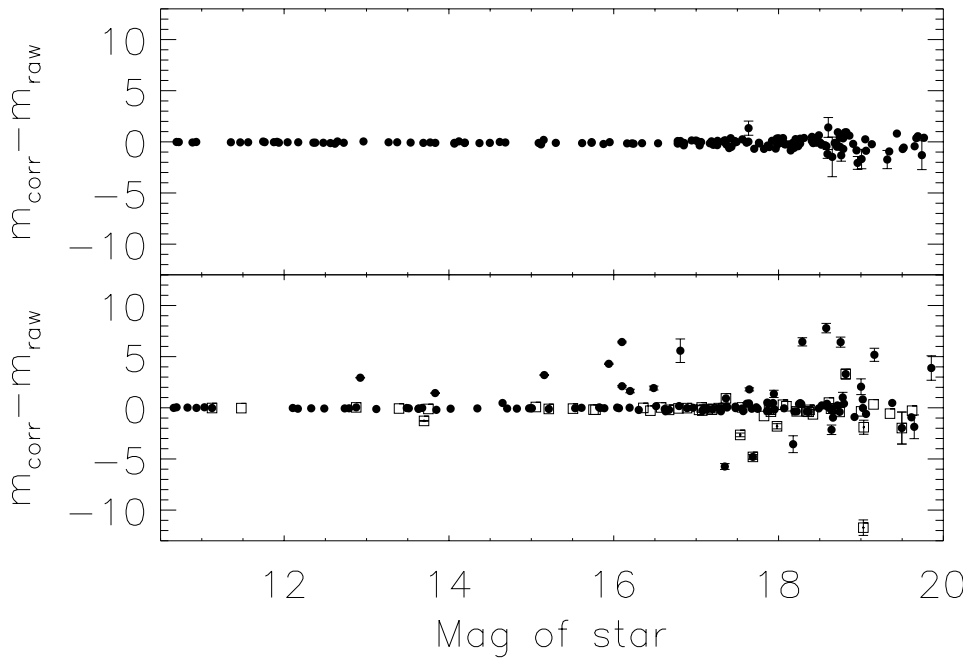


*Figure 3.* Magnitude offsets (in mmag) between photometry from corrected and raw images. Top: Check stars without close ghosts. Bottom: Contaminated stars with ghosts inside the aperture radius (fat dots) and ghosts inside the sky annulus (squares).  $1\text{-}\sigma$  (standard deviation) error bars are plotted for magnitude offsets larger than 1 mmag. The axis of abscissas gives approximate magnitudes.

several stars. *Difference light curves* between cross-talk corrected and raw light curves were calculated. Three sets of stars were selected: *set A* with 134 stars positioned on the CCD such that a ghost from a star on the other CCD half would be inside the stellar aperture, *set B* with 57 stars having ghosts outside the stellar aperture but inside the sky annulus, and *set C* with 165 uncontaminated *check stars*.

### 5.1. MAGNITUDE OFFSETS

The telescope's auto guiding was good and the relative shifts of the stars in the 108 images were below 2 pixels ( $0.''8$ ) in vertical and horizontal directions. A ghost close to a star may therefore add an offset to the stellar magnitude – negative, if the sky-background determination is affected, and positive if only the stellar counts are contaminated. The effect of cross-talk correction on the photometry is seen in Figure 3 where mean values of the 109 measurements in each difference light curve (corrected-raw) are given. The top panel shows non-contaminated check stars from set C and the bottom panel shows contaminated stars from set A and B. The correction has no effect on the photometry for most stars, contaminated or not. Some 10% of the contaminated stars have significant (but typically below

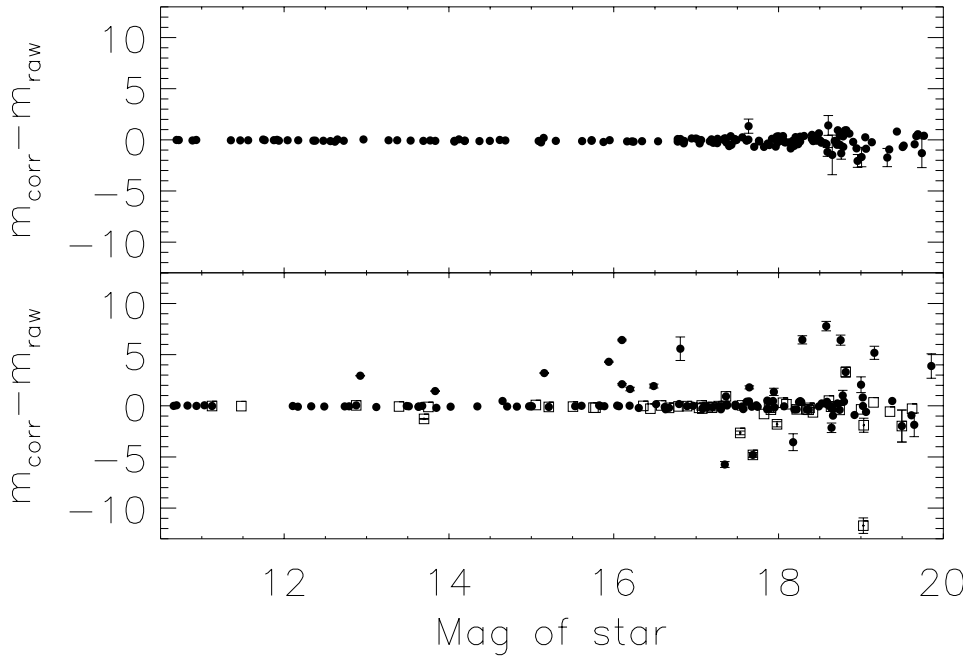


Figure 4. Differences in light curve r.m.s. scatter (in mmag, cross-talk corrected minus raw light curves), given in magnitudes for the 165 check stars (top panel) and 134 stars contaminated inside the aperture (bottom panel). Plus symbols indicate positions of stars #4 and #5 (Table III).

5 mmag) offsets in the photometry. Affected stars with negative offsets are, as expected, mostly stars contaminated in the sky annulus (boxes), while stars with positive offsets mostly are stars contaminated inside the aperture radius (fat dots).

The majority of the stars which are contaminated inside the sky annulus are not affected by the correction, which indicates that the sigma-clipping sky-determination by MOMF is robust against such a contamination. That the check stars are not affected by the correction, provides a check on the correction procedure – indeed, only the relevant pixels are corrected. The fact that so few of the contaminated stars are affected shows that the cross-talk signal only matters under certain conditions. In our case, as we show below, must the source of the cross-talk ghost be saturated and extended over several pixels in order to affect even the fainter stars in our sample.

## 5.2. SCATTER IN TIME SERIES

Cross-talk contamination of photometry may not only be systematic – the cross-talk is coupled with meteorological conditions (see below). The mean magnitude offsets in Figure 3 may, therefore, be considerably smaller than offsets in individual measurements, while the light curves r.m.s. scatter may be significantly increased.

TABLE III

De-correlation of seven light curves. *IDs 1–5* are constant stars from set A and *IDs 6–7* are check stars from set C. Median magnitudes of the respective time series are given in col. 2, magnitude offsets after cross-talk correction in col. 3 and r.m.s. scatter in cols. 4 and 8. De-correlation coefficients are given for CCD position  $x, y$  and seeing, for raw (cols. 5–7) and cross-talk corrected (cols. 9–11) data

ID	m (mag)	$\Delta m$ (mmag)	Raw data ( $10^{-3}$ )				Corrected data ( $10^{-3}$ )			
			$\sigma$	x	y	Seeing	$\sigma$	x	y	Seeing
1	16.1	$2.1 \pm 0.8$	4.23	3.4	-0.3	2.5	4.25	2.7	-0.2	2.9
2	14.7	$0.5 \pm 0.3$	2.67	-1.3	-1.4	0.3	2.61	-0.8	-1.3	0.6
3	12.9	$0.1 \pm 0.1$	3.76	-0.2	1.0	-0.4	3.65	0.0	1.1	0.2
4	16.7	$67.1 \pm 11.0$	8.02	-2.5	-0.3	0.5	8.35	-0.2	-1.3	2.0
5	17.1	$25.5 \pm 3.9$	11.23	23.8	3.1	-8.2	10.55	-0.3	2.9	0.5
6	15.1	$-0.3 \pm 0.3$	2.93	-1.3	2.4	0.3	2.91	-1.5	2.3	0.4
7	16.9	$0.1 \pm 1.0$	8.41	4.6	7.2	2.2	8.37	4.4	7.2	1.9

Figure 4 shows changes in r.m.s. scatter for light curves from corrected and raw science images. The bottom panel is for contaminated stars from set A and the top panel is for check stars in set C. Comparison between these two panels suggests that scatter may be slightly higher in light curves of contaminated stars as compared to the check stars. Only stars fainter than 15th mag are affected, and this only slightly. The reason for such a small effect may be the stable observing conditions that night.

### 5.3. CORRELATION EFFECTS ON TIME SERIES

Cross-talk effects on photometry are, as mentioned above, coupled with observing conditions. For instance, seeing variations change the flux in central pixels of stellar images and thus also the single-pixel contamination; pointing offsets, flexure or guiding errors shift stars in or out of ghosts, especially for horizontal shifts, which are doubled by the mirrored displacement of the ghosts, finally high sky levels due to moon/twilight may drown the contamination.

To check for such effects we selected five contaminated stars, which were constant and isolated from other stars, and two check stars from set C. Time series from corrected and raw images were de-correlated with stellar shifts in  $x$ - and  $y$ -positions and with seeing following the procedure in Freyhammer et al. (2001). Table III gives the results. Only the stars #4 and #5 are clearly affected by cross-talk correction as seen on the large magnitude offsets between the corrected and non-corrected data (col. 3). In the case of star #5, the cross-talk correction also reduces the r.m.s. scatter slightly by removing a strong correlation with  $x$ -position and to some extent also with seeing. For star #4 the correction has no clear effect

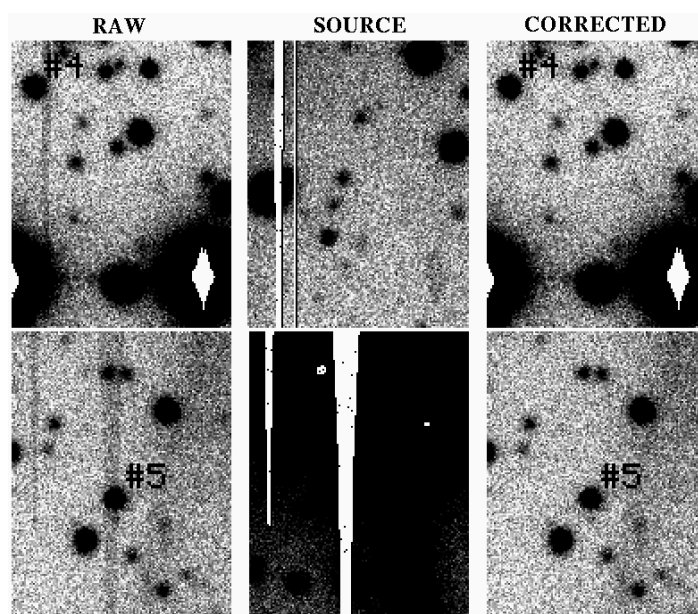


Figure 5. Image sections with stars #4 (top) and #5 (bottom) before (RAW) and after (CORRECTED) cross-talk correction. Inverted gray scale with cuts between 200 and 370 ADU. The middle panels (SOURCE) show the source signal for the cross-talk with saturated pixels shown in white. Note the ghosts from charge-blooming ‘spikes’, and from the saturated star in the top panels.

on the r.m.s. scatter or the correlation coefficients, though some interchanges are seen among the coefficients.

Why are the effects so different for the five stars? Figure 5 shows image sections with stars #4 and #5 before and after correction. The middle panels in the figure show the corresponding, mirrored real signal sections. In the RAW panels it is seen that ghosts from pixels with charge blooming clearly contaminate the stars #4 and #5 inside their aperture radii. No effect is seen for stars #1–#3, and from Figure 5 we realise why: only saturated pixels produce visible ghosts, like the saturated star at the lower right part of the top panels, which leaves a ghost in the middle panel labelled ‘Source’. Only the saturated pixels are seen in the ghost, so contamination by stars that are not saturated is negligible for this camera. Stars #1 and #2 are both contaminated by images that are not saturated, while star #3 is much too bright to be affected on the mmag-level by the relatively small contamination.

#### 5.4. FORS1 – CORRECTED CALIBRATION FRAMES

We used Equation (6) to recover the three FORS1 calibration images (Section 3) from cross-talk, only considering the AB cross-talk term. The correction properly removes all ghosts, except in the  $5\times$  full-well image.

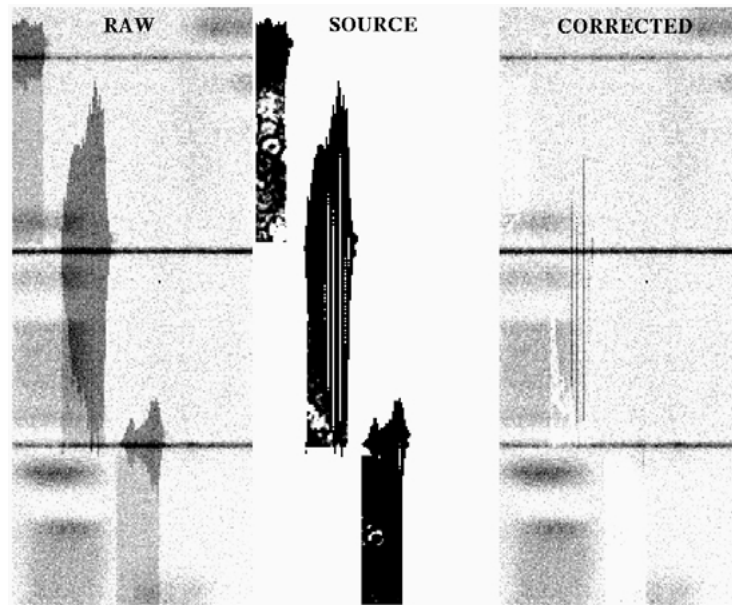


Figure 6. Correction of AB cross-talk of the  $5\times$  full-well image. Inverted gray scale with cuts of 200–240 ADU (63–66 kADU for the middle panel). (RAW) Ghosts in image-quadrant B, (SOURCE) three saturated slit images in the A quadrant (swapped columns), (CORRECTED) the corrected B-quadrant section. See text for details on the correction. Optical reflections are seen mainly to the left of the ghosts, and 3 horizontal MOS-panel spacings are seen.

Figure 6 shows image sections with AB ghosts from three saturated slits in the  $5\times$  full-well image, before and after correction (left and right panels). Unexpected structures are seen in the saturated slit images (middle panel): *patches* of charge blooming are seen on top of all slit images, which is probably an effect of reflected light from the spacings between the MOS sliding panels; in the patch over the central slit are 5 apparently ‘dead’ columns with zero counts; and *fringes* of 92–100% digital saturation are seen in regions of the slit images that are outside the charge blooming patches. The blooming patches and the ‘dead’ columns both produce ghosts (RAW panel) with the maximum cross-talk predicted by Equation (6) and do, therefore, not stand out from one another. The fringe regions give ghosts of half that level (in spite of that the slits were also overexposed) without fringes.

Such effects could be related to a poor CTE at high charge, or the controller could have a blooming protection (see e.g. Neely and Janesick (1993) for a description on antiblooming) that neutralises charges during the charge-transfer phases, etc. Since the cross-talk ghosts do not match their sources, we cannot properly correct this image (CORRECTED).

## 6. Discussion and conclusion

The difficulties in removal of cross-talk contamination from science images are mainly concentrated in the analysis and measurement of the contribution. The procedure fails in case of strong saturation, i.e. several times full well. Changing the gain, e.g. from low to high gain, does not alter the cross-talk amplitudes, when the cross-talk originates from the CCD itself rather than from the ADCs electronic circuits. The gain does, however, change the region from numerical saturation to full well. If the ADC saturates before full well is reached, this region is not visible and cross-talk will then contribute from an immeasurable source signal. The narrower this region is, i.e. the more the full-well capacity is used before saturation, the better the correction procedure becomes. The immeasurable region may be accessed if a considerable effort is made to fit PSFs to the wings of saturated stars, or by predicting the exposure levels from magnitude offsets to non-saturated stars.

All calibration images could be obtained in daytime, because the two re-imaging instruments allow to insert masks in the telescopes focal planes. We have only analysed imaging instruments, but the found cross-talk effects may also apply to spectroscopic images with emission lines, such as wavelength calibration images. For echelle spectra, in particular fiber-fed spectrographs with a calibration lamp in a second fiber, the tracing and extraction of orders could be affected by ghost signal in the local background.

In analysing the effect of CT in real science data, we find for a single star that the cross-talk strongly correlates with the relative CCD pixel position and seeing in photometric data. This suggests that, in some cases, cross-talk effects on time-series photometry may be reduced through de-correlation. Strong effects from the cross-talk are seen in the photometry, but only from saturated objects, which is due to the moderate cross-talk amplitude of  $10^{-4}$ , but we are aware of other recent CCD cameras, where the level is  $10^{-3}$ . At such amplitudes, the contamination is a serious problem for most applications.

In conclusion, a procedure for mapping and efficient removal of cross-talk has been given after successful application on two- and four-port data. We have shown the significance of the signal, mapped it inside and above the CCDs dynamical ranges, and described the effects of the corrections on high-precision time-series photometry and contaminated images.

## Acknowledgements

A part of this research was carried out in the framework of the project 'IUAP P4/05' financed by the Belgian DWTC/SSTC and a part of the work was done under a

studentship at Nordic Optical Telescope\* (LMF). This work has been supported by the Belgian Fund for Scientific Research (FWO) and by the Flemish Ministry for Foreign Policy, European Affairs, Science and Technology, under contract BIL 99/2, and by the Danish Natural Science Research Council through the center for Ground Based Observational Astronomy.

### References

- Arentoft, T., Sterken, C., Knudsen, M. R. et al.: 2001, *A&A* **380**, 599.
- ESO: 1999, 'FORS User Manual', *User Manual*, European Southern Observatory.
- Freyhammer, L. M., Andersen, M. I. and Petersen, J. O.: 1999, in L. Szabados and D. Kurtz (eds), *ASP Conf. Series*, Vol. 203, p. 252.
- Freyhammer, L. M., Arentoft, T. and Sterken, C.: 2001, *A&A* **368**, 580.
- Hoffberg, M.: 1996, in 'CCD World', Mess. on 5 March 1997, <http://www.not.iac.es/CCD-world/>.
- Jorden, P.: 1997, in 'CCD World', Mess. on 5 March 1997, <http://www.not.iac.es/CCD-world/>.
- Kjeldsen, H. and Frandsen, S.: 1992, *PASP* **104**, 413.
- Marshall, S.: 1995, in 'CCD World', Mess. on 13 September, <http://www.not.iac.es/CCD-world/>.
- Mackay, C. D.: 1986, *ARA&A* **24**, 255.
- Mackay, C. D., Tubbs, R. N., Bell, R. et al.: 2001, in M. M. Blouke, J. Canosa and N. Sampat (eds), *SPIE Proceedings 4306*, pp. 299–307.
- McLean, I. S.: 1997, *Electronic Imaging in Astronomy*, Wiley & Sons.
- Neely, A. W. and Janesick, J. R.: 1993, *PASP* **105**, 1330.
- Sørensen, A. N. and Andersen, M. I.: 1997, 'Properties of W7-(0,0)', *Test Report*, Copenhagen University Observatory.

\* Nordic Optical Telescope is operated on the island of La Palma jointly by Denmark, Finland, Iceland, Norway, and Sweden, in the Spanish Observatorio del Roque de los Muchachos of the Instituto de Astrofísica de Canarias.